ORGANIC LETTERS

2011
Vol. 13, No. 17
4588–4591

Quinoxaline-Embedded Polyacenoquinone Esters: Synthesis, Electronic Properties, and Crystal Structure

Teh-Chang Chou,*,† Kuen-Cheng Lin,† Masaru Kon-no,‡ Chih-Ching Lee,† and Teruo Shinmyozu‡

Department of Applied Chemistry, Chaoyang University of Technology, Wufong, Taichung, 41369, Taiwan, and Institute for Materials Chemistry and Engineering (IMCE), Kyushu University, 6-10-1 Hakozaki, Fukuoka 812-8581, Japan

tcchou@cyut.edu.tw

Received July 3, 2011

ABSTRACT

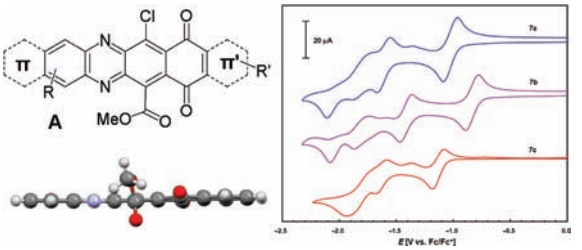

The development of an expedient synthesis toward quinoxaline ring-embedded polyacenoquinone esters with the generic structure A is demonstrated by the synthesis of penta- and hexacenoquinone esters. They are potential n-type small molecules, capable of undergoing successive reductions and self-assembling in face-to-face π-stacks.

Quinoxalines and their derivatives are important members of heterocyclic compounds that have been widely applied in many fields. They display diverse biological activity and have been used for the design of pharmaceuticals.[1] The spectroscopic properties of quinoxaline-embedded chromophores are particularly attractive because of the easy modification of the basic skeleton for the design of functional materials, such as sensing molecules[2] and photo- and electroluminescent molecules.[3,4]

Recently, considerable interest in aza-substituted acenes has emerged because of their possible application in developing useful *n*-type (electron-transporter) semiconductor material.[5] Compared to hydrocarbon analogues, heteroacenes containing imine nitrogen atoms (−N═) generally have less negative reductive potential and higher electron affinity.[5,6] When integrating the 1,4-quinone ring or attaching electron-withdrawing groups, such as the halogen or the cyano moiety, azaacenes could boost their electron affinity[7] and gain a better chance to form a π-stack in a face-to-face structure via a hydrogen-bond-assisted

† Chaoyang University of Technology.
‡ Kyushu University.

(1) (a) Romeiro, N. C.; Aguirre, G.; Hernandez, P.; Gonzalez, M.; Cerecetto, H.; Aldana, I.; Perez-Silanes, S.; Monge, A.; Barreiro, E. J.; Lima, L. M. *Bioorg. Med. Chem.* **2009**, *17*, 641–652. (b) Bräse, S.; Gil, C.; Knepper, K. *Bioorg. Med. Chem.* **2002**, *10*, 2415–2437.

(2) (a) Beaudoin, D. S.; Obare, S. O. *Tetrahedron Lett.* **2008**, *49*, 6054–6057. (b) Chauhan, S. M. S.; Bisht, T.; Garg, B. *Tetrahedron Lett.* **2008**, *49*, 6646–6649. (c) Kruger, P. E.; Mackie, P. R.; Nieuwenhuyzen, M. *J. Chem. Soc., Perkin Trans. 2* **2001**, 1079–1083.

(3) (a) Son, H.-J.; Han, W.-S.; Wee, K.-R.; Yoo, D.-H.; Lee, J.-H.; Kwon, S.-N.; Ko, J.; Kang, S. O. *Org. Lett.* **2008**, *10*, 5401–5404. (b) Mancilha, F. S.; DaSilveira Neto, B. A.; Lopes, A. S.; Moreira, P. F., Jr.; Quina, F. H.; Gonçalves, R. S.; Dupont, J. *Eur. J. Org. Chem.* **2006**, 4924–4933.

(4) (a) Karastatiris, P.; Mikroyannidis, J. A.; Spiliopoulos, I. K.; Kulkarni, A. P.; Jenekhe, S. A. *Macromolecules* **2004**, *37*, 7867–7878. (b) Okamoto, T.; Terada, E.; Kozaki, M.; Uchida, M.; Kikukawa, S.; Okada, K. *Org. Lett.* **2003**, *5*, 373–376. (c) Thomas, K. R. J.; Lin, J. T.; Tao, Y.-T.; Chuen, C.-H. *Chem. Mater.* **2002**, *14*, 2796–2802.

(5) (a) Bunz, U. H. F. *Chem.—Eur. J.* **2009**, *15*, 6780–6789. (b) Richards, G. J.; Hill, J. P.; Subbaiyan, N. K.; D'Souza, F.; Karr, P. A.; Elsegood, M. R. J.; Teat, S. J.; Mori, T.; Ariga, K. *J. Org. Chem.* **2009**, *74*, 8914–8923. (c) Winkler, M.; Houk, K. N. *J. Am. Chem. Soc.* **2007**, *129*, 1805–1815. (d) Stöckner, F.; Beckert, R.; Gleich, D.; Birckner, E.; Günther, W.; Görls, H.; Vaughan, G. *Eur. J. Org. Chem.* **2007**, 1237–1243.

10.1021/ol2017774
Published on Web 08/10/2011

Scheme 1. Synthesis of **A** (**7a**–**c**)

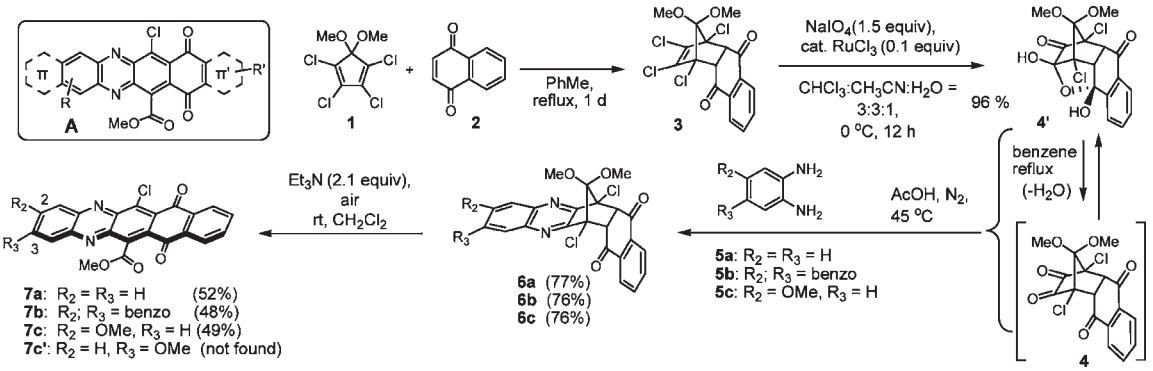

intermolecular $\pi-\pi$ stacking interaction.[8] Theoretically, a cofacial π-stacking structure is expected to provide more efficient orbital overlap and thereby facilitate charge carrier transport.[9] Search for stable, amendable azaacenes with high electron affinity as building blocks for constructing conjugated polymer semiconductors has also been actively demonstrated.[10]

In this context, we developed a strategy for expedient synthesis of quinoxaline-embedded polyacenoquinone esters with the generic structure **A** (Scheme 1) via the process demonstrated by the preparation of pentacenoquinone esters **7a**,**c** and hexacenoquinone ester **7b**. Molecules of **A** are composed of three basic aromatic ring systems of electron-accepting nature, namely 1,4-benzoquinone, benzene with electron-withdrawing substituents ($-CO_2Me$, $-Cl$), and quinoxaline. Accordingly, molecules of **A** are expected to have an electronic structure exhibiting high electron affinity, planar geometry, and a tendency to self-assemble in the solid state by cofacial packing arrangement via $\pi-\pi$ stacking interaction. We herein report the results of synthetic exploration, the electrochemical and optical properties, and the crystal structures.

The synthesis started from the Diels–Alder adduct **3**[11,12] of 1,2,3,4-tetrachloro-5,5-dimethoxycyclopentadiene (**1**)[13] and naphthalene-1,4-dione (**2**), followed basically by three key operations as shown in Scheme 1: (1) the ruthenium-promoted $NaIO_4$ oxidation,[12,14] (2) the condensation reaction of an α-diketone with an arene-1,2-diamine,[15] and (3) the transformation involving enolization, oxidation, and the Grob-type fragmentation that occurred consecutively in one pot.[16,17] Accordingly, when adduct **3** was subjected to the $NaIO_4$ oxidation, the reaction yielded a product showing a rather complex ^1H NMR spectrum and an IR spectrum containing absorption bands due to the hydroxyl and carbonyl groups. This product was proved to be the desired α-diketone **4** in its monohydrate form **4′**.[18] Condensation of α-diketone **4** or **4′** (or both together) with benzene-1,2-diamine (**5a**), naphthalene-2,3-diamine (**5b**), or 4-methoxybenzene-1,2-diamine (**5c**) in AcOH at 45 °C under N_2 atmosphere afforded the corresponding quinoxalino-fused derivatives **6a**, **6b**, or **6c**.[19]

As expected, stirring a solution of **6a** or **6b** in CH_2Cl_2 with triethylamine in the presence of air (O_2), successive enolization, oxidation, and fragmentation occurred to furnish the colored pentacenoquinone ester **7a** (bright yellow, 52%) and hexacenoquinone ester **7b** (dark brown, 48%).[19] In principle, the fragmentation of **6c** was expected to yield two isomeric fragmentation products, in which the methoxy

(6) (a) Tonzola, C. J.; Alam, M. M.; Kaminsky, W.; Jenekhe, S. A. *J. Am. Chem. Soc.* **2003**, *125*, 13548–13558. (b) Miao, S.; Brombosz, S. M.; Schleyer, P. v. R.; Wu, J. I.; Barlow, S.; Marder, S. R.; Hardcastle, K. I.; Bunz, U. H. F. *J. Am. Chem. Soc.* **2008**, *130*, 7339–7344.

(7) (a) Liang, Z.; Tang, Q.; Liu, J.; Li, J.; Yan, F.; Miao, Q. *Chem. Mater.* **2010**, *22*, 6438–6443. (b) Tang, M. L.; Oh, J. H.; Reichardt, A. D.; Bao, Z. *J. Am. Chem. Soc.* **2009**, *131*, 3733–3740. (c) Kuo, M. Y.; Chen, H. Y.; Chao, I. *Chem.—Eur. J.* **2007**, *13*, 4750–4758. (d) Sakamoto, Y.; Suzuki, T.; Kobayashi, M.; Gao, Y.; Fukai, Y.; Inoue, Y.; Sato, F.; Tokito, S. *J. Am. Chem. Soc.* **2004**, *126*, 8138–8140.

(8) (a) Weng, S.-Z.; Shukla, P.; Kuo, M.-Y.; Chang, Y.-C.; Sheu, H. -S.; Chao, I.; Tao, Y.-T. *Appl. Mater. Interfaces* **2009**, *1*, 2071–2079. (b) Moon, H.; Zeis, R.; Borkent, E.-J.; Besnard, C.; Lovinger, A. J.; Siegrist, T.; Kloc, C.; Bao, Z. *J. Am. Chem. Soc.* **2004**, *126*, 15322–15323.

(9) (a) Curtis, M. D.; Cao, J.; Kampf, J. W. *J. Am. Chem. Soc.* **2004**, *126*, 4318–4328. (b) Cornil, J.; Lemaur, V.; Calbert, J. P.; Brédas, J. L. *Adv. Mater.* **2002**, *14*, 726–729.

(10) (a) Mastalerz, M.; Fischer, V.; Ma, C.-Q.; Janssen, R. A. J.; Bäuerle, P. *Org. Lett.* **2009**, *11*, 4500–4503. (b) Bangcuyo, C. G.; Ellsworth, J. M.; Evans, U.; Myrick, M. L.; Bunz, U. H. F. *Macromolecules* **2003**, *36*, 546–548. (c) Jonforsen, M.; Johansson, T.; Ingana1, O.; Andersson, M. R. *Macromolecules* **2002**, *35*, 1638–1643. (d) Jandke, M.; Strohriegl, P.; Berleb, S.; Werner, E.; Brütting, W. *Macromolecules* **1998**, *31*, 6434–6443.

(11) Chou, T.-C.; Hong, P.-C.; Wu, Y.-F.; Chang, W.-Y.; Lin, C.-T.; Lin, K.-J. *Tetrahedron* **1996**, *52*, 6325–6338.

(12) The simpler Diels–Alder adduct derived from 1,4-benzoquinone and **1** was not applicable. The ruthenium-promoted $NaIO_4$ oxidation occurred exclusively at the endione C=C bond.

(13) Khan, F. A.; Prabhudas, B.; Dash, J. *J. Prakt. Chem.* **2000**, *342*, 512–517.

(14) (a) Khan, F. A.; Dash, J. *J. Am. Chem. Soc.* **2002**, *124*, 2424–2425. (b) Khan, F. A.; Prabhudas, B.; Dash, J.; Sahu, N. *J. Am. Chem. Soc.* **2000**, *122*, 9558–9559.

(15) (a) Chou, T.-C.; Liao, K.-C.; Lin, J.-J. *Org. Lett.* **2005**, *7*, 4843–4846. (b) Chou, T.-C.; Lin, K.-C.; Wu, C.-A. *Tetrahedron* **2009**, *65*, 10243–10257. (c) Chou, T.-C.; Liao, K.-C. *Tetrahedron* **2011**, *67*, 236–249.

(16) Chou, T.-C.; Hsu, C.-J.; Chen, J.-Y. *J. Chin. Chem. Soc.* **2004**, *51*, 167–174.

(17) (a) Mehta, G.; Padma, S.; Venkatesan, K.; Be gum, N. S.; Moorthy, J. N. *Indian J. Chem.* **1992**, *31B*, 473–482. (b) Marchand, A. P.; Alihodzic, S.; Shukla, R. *Synth. Commun.* **1998**, *28*, 541–546.

(18) Dehydration of **4′** under azeotropic reflux with benzene gave the hygroscopic α-diketone **4**, indicated by its symmetry-reflect ^1H NMR spectrum and the absence of OH absorption in the IR spectrum.

group is trans (**7c**) or cis (**7c′**) to the methoxycarbonyl group (Scheme 1). However, only one regioisomer was found. Discriminating between two regioisomers could only be made by X-ray crystallography (vide infra), which indicated that *trans*-isomer **7c** was the fragmentation product.

Plausible mechanism of the formation of **7** from **6** keyed upon the Grob-type fragmentation is outlined in Scheme 2. The methano-bridged naphthoquinone **B**, derived from **6** via successive enolization and oxidation, would fragment to generate intermediate **C** by pathway i, followed by the elimination of CH_3Cl to yield ester **7**.[16,17] The fragmentation is driven by the relief of ring strain and aromatization and assisted by the push−pull setup for electrons to flow from MeO to C=O groups relayed by the enone C=C bond. Because of the incorporation of the imine groups that are properly located to apply extra electron-pull force, **B** is expected to undergo fragmentation more efficiently with additional pathway ii (Scheme 2). The high regioselectivity displayed by conversion of **6c** to **7c** is possibly attributable to the electron-donating substituent (e.g., OMe) at the quinoxaline ring, which weakens the electron-pull force of its para-located imine group and destabilizes the negative charge developed therein. Consequently, the cleavage of bridging C−C bond occurs preferentially to give the intermediate **C** (R_2 = OMe) as shown in Scheme 2, leading to the formation of observed *trans*-isomer **7c**.

Scheme 2. Plausible Mechanism for the Fragmentation of Quinoxaline-Embedded Naphthoquinone **B**

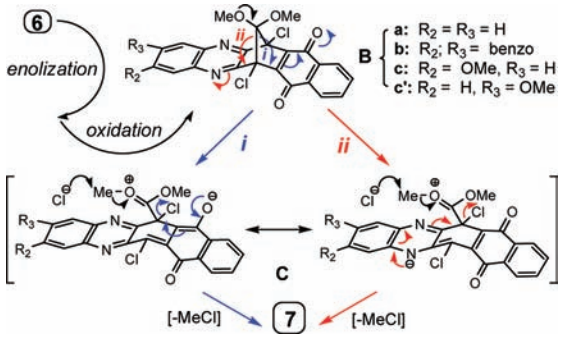

The electronic structures and the electron-accepting characteristics of **7a**−**c** were examined using both experimental and computational methods. Their cyclic voltammograms (CVs) are shown in Figure 1,[20] and the resultant redox potentials, together with the values of LUMO energy obtained from computation (Figure S1 and Table S1 in the Supporting Information)[21] and experiments are summarized in Table 1. The CVs of **7a** and **7b** are very similar, displaying three reversible and one irreversible redox waves (E^4_{pc}), while that of **7c** shows only two reversible (E^1 and E^2) and one irreversible redox waves (E^3) without the fourth redox wave. The reversible redox waves indicate that **7a** and **7b** could undergo a three-electron redox process and therefore be potential candidates for inclusion in an electron-transporting layer of an OLED. However, the irreversible redox wave at high voltage (E^4_{pc}) is possibly caused by the presence of methoxycarbonyl, which forms irreversible electron traps on the electrode surface during the reduction process.

The first reduction peak is attributed to the uptake of one electron to form a radical-anion $[\mathbf{A}]^{\bullet-}$ (**A** = **7a** or **7b** or **7c**). From the halfwave reduction potential vs ferrocenium/ferrocene,[7d,22] the energy levels for LUMO of **7a** **7b**, and **7c** are estimated to be −3.77, −3.96, and −3.67 eV, respectively, in agreement with the calculated energy levels (Table 1). The elevating of the LUMO levels in the order of **7b** < **7a** < **7c** reflects the extent of π-conjugation and the effect of electron-donating substituent (OMe). As compared with other nitrogen heterocycles, such as quinoxaline, acridine, and phenazine,[6b,23] **7a**−**c** have greater electron uptake ability. In addition, the ground-state molecular orbitals (Figure S1b, Supporting Information) show that the HOMO and LUMO of **7a**, **7b**, and **7c** are greatly localized on the diazaacene moiety, and the benzoquinone ring blocks the π-conjugation. This may imply that the diazaacene nucleus in **7a**−**c** plays a more significant role of electron uptake in the initial reduction process and the electron delocalization within molecules is ineffectual, reflecting on the observed well-defined redox waves.

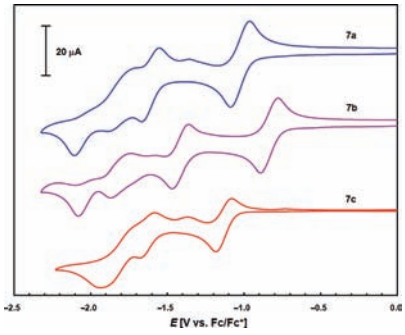

Figure 1. Cyclic voltammograms of **7a**, **7b**, and **7c** in CH_2Cl_2.

(19) Under this condition (AcOH as solvent), a small amount of the corresponding tautomers of **6a**−**c** was inevitably formed. However, these tautomers underwent oxidation−fragmentation to form the corresponding acenoquinone esters at higher temperature or during isolation, suggesting that the condensation reaction could be combined with Grob-type fragmentation to give the final product in a one-pot operation.

(20) The CVs of **7a**−**c** were also recorded in THF at lower concentrations (0.3−0.5 mM). The E^1 and E^2 reduction waves are reversible and similar to those recorded in CH_2Cl_2, but the E^3 peak was found to be irreversible and the E^4 peak was not observed (see Figure S2b and Table S2b, Supporting Information). Since the differences between cathodic/anodic peak potentials (E_{pc}/E_{pa}) in THF are often larger than the those in CH_2Cl_2, the third and fourth peaks were probably overlapped.

(21) (a) Head-Gordon, M.; Pople, J. A. *Chem. Phys. Lett.* **1988**, *153*, 503–506. (b) Becke, A. D. *J. Chem. Phys.* **1993**, *98*, 1372–1377.

(22) D'Andrade, B. W.; Datta, S.; Forrest, S. R.; Djurovich, P.; Polikarpov, E.; Thompson, E. *Org. Electron.* **2005**, *6*, 11–20.

(23) (a) Kobayashi, T.; Kobayashi, S. *Eur. J. Org. Chem.* **2002**, 2066–2073. (b) Doernera, T.; Rolf Gleiter, R.; Neugebauer, F. A. *Eur. J. Org. Chem.* **1998**, 1615–1623. (c) Ames, J. R.; Houghtaling, M. A.; Terrian, D. L. *Electrochim. Acta* **1992**, *37*, 1433–1436. (d) Wiberg, K. B.; Lewis, T. P. *J. Am. Chem. Soc.* **1970**, *92*, 7154–7160.

Table 1. Redox Potentials (V vs Fc/Fc^+), Optical Properties (λ_{max}, λ_{em}), and the MO Energies (eV) for **7a**, **7b**, and **7c**

	$E^1_{1/2}(0/-1)$ (E^1_{pc}; E^1_{pa})[a]	$E^2_{1/2}(-1/-2)$ (E^2_{pc}; E^2_{pa})[a]	$E^3_{1/2}(-2/-3)$ (E^3_{pc}; E^3_{pa})[a]	$E^4_{pc}(-3/-4)$[a]	λ_{max}/nm (log ε)[b]	λ_{edge}/nm	λ_{em}/nm[b,c]	LUMO	HOMO
7a	−1.03	−1.62	−1.80		328 (4.4)	380	523	−3.77[g]	−7.03[h]
	(−1.08; −0.98)	(−1.66; −1.58)	(−1.88; −1.73)	−2.09	382[d]			−3.61[i]	−6.86[i]
7b	−0.84	−1.42	−1.82		367 (4.6)	480	624	−3.96[g]	−6.54[h]
	(−0.88; −0.80)	(−1.46; −1.38)	(−1.85; −1.76)	−2.07	543[d]			−3.79[i]	−6.26[i]
7c	−1.13	−1.63			338 (4.6)	390	508	−3.67[g]	−6.85[h]
	(−1.17; −1.09)	(−1.67; −1.60)	(−1.93; −1.73[e])	[f]	431[d]			−3.43[i]	−6.65[i]

[a] Conditions: sample (1 mmol/dm^3) in 0.1 mol/dm^3 n-Bu_4NPF_6/CH_2Cl_2 solution; temperature, 300 K; working electrode, glassy carbon; reference electrode, $Ag/AgNO_3$ (0.01 mol/dm^3 in 0.1 mol/dm^3 n-Bu_4NPF_6/CH_3CN solution); counter electrode, Pt; scan rate, 100 mV/s for **7a** and **7b**, 50 mV/s for **7c**. [b] Measured at the concentration of 1×10^{-5} M in $CHCl_3$. [c] Excitation wavelength (λ_{ex}): **7a**, 338 nm; **7b**, 365 nm; **7c**, 338 nm. [d] Charge transfer band: **7a**, 375−450 nm; **7b**, 490−600 nm; **7c**, 400−490 nm. [e] Estimated value due to the shoulder peak. [f] Not observed in the electrochemical window for CH_2Cl_2. [g] Estimated with reference to ferrocenium/ferrocene (4.80 eV). [h] Estimated according to the equation $E_{HOMO} = (E_{LUMO} + E_{\lambda edge})$ eV, where E_{LUMO} is the CV experimental value. [i] Calculated by the DFT [(B3LYP/6-311+G(d,p)//B3LYP/6-31G(d)] calculations.

The absorption and photoluminescence (PL) spectra of **7a**−**c** (Figure S3 in Supporting Information) were recorded in chloroform, and the data are listed in Table 1. All compounds exhibit a prominent absorption band appearing at 300−400 nm ascribed to the π,π^* transition,[10,24] and weak bands of lower energy (350−500 nm) attributable to the charge-transfer (CT) character (Figure S3a, Supporting Information). The peak wavelengths (λ_{max}) and intensity reflect the substituent effect and the extent of π-conjugation. The HOMO energy levels for **7a**, **7b**, and **7c** were determined to be −7.03, −6.54, and −6.85 eV, respectively, in agreement with the calculated energies for their HOMOs (Table 1 and Table S1, Supporting Information). The PL spectra of **7a** and **7c** are very weak relative to that of **7b** (Figure S3b, Supporting Information). As indicated by the normalized PL spectra (Figure S3c, Supporting Information), the emission maximum is red-shifted from 508 nm for **7c** to 523 nm for **7a** and then to 624 nm for **7b**.

The ORTEP drawings of **7a** and **7c** are shown in Figure S4 in the Supporting Information. The molecular structure of **7a** is planar, and that of **7c** is slightly twisted (ca. 12°). The plane of carboxyl group stretches out almost perpendicular to the plane of aryl ring. Both **7a** and **7c** adopt the cofacial slipped π-stacking structure as shown in Figure 2, which also reveals the notable role played by the polarized methoxy groups (OCH_3) in the molecular packing.[15b,c] Molecules of **7a** align in a head-to-head style with an interplanar distances of 3.39 Å (centroid-to-centriod distance 5.13 Å) and linked by the intermolecular C−H···O hydrogen bonds (2.63 Å), Figure 2a. Conversely, molecules of **7c** assemble in a head-to-tail manner, and the analogous C−H···O hydrogen bonds (2.66 Å) interlock two molecules to form a stacked dimeric structure, in which the interplanar distance is 3.34 Å (centroid-to-centriod distance 4.41 Å). As shown in Figure 2b, the neighboring dimeric units are further stacked with an interplanar distance of 3.54 Å (centroid-to-centriod distance 4.47 Å) and further secured by C−H···π interactions between the polarized OCH_3 and phenyl ring ($d_{H\ldots\pi}$ = 3.26 Å).

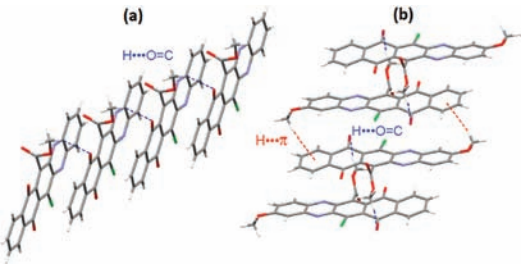

Figure 2. Cofacial π-stacking structures: (a) **7a**, (b) **7c**.

In conclusion, we have successfully developed a versatile synthetic route toward the quinoxaline-embedded polyacenoquinone esters **7a**−**c**. Compounds **7a**−**c** display well-defined, reversible redox waves in the initial reduction process, indicative of the *n*-type (electron-transporter) doping nature. The X-ray diffraction data of **7a** and **7c** reveal cofacial π−π stacking between two neighboring molecules, helpful to charge carrier transport. In a synthetic application perspective, the inherited substituents in this new family of polyacenoquinone esters are exploitable to make them valuable synthetic precursors of quinoxaline-embedded polyacenyl derivatives.

Acknowledgment. This work was financially supported by the National Science Council of Taiwan. T.-C. C thanks IMCE, Kyushu University, for an invitation as a visiting foreign researcher during July and August, 2010.

Supporting Information Available. Experimental procedures with characterization data and spectra for new compounds; table and figure of DFT calculated MO energies; absorption/emission spectra for compounds **7a**−**c**; ORTEP drawings and X-ray crystallographic information files (CIF) for **7a** and **7c**. This material is available free of charge via the Internet at http://pubs.acs.org.

(24) (a) Waluk, J.; Grabowska, A.; Pakulstroka, B. *J. Lumin.* **1980**, *21*, 277–291. (b) Imes, K. K.; Ross, I. G.; Moomaw, W. R. *J. Mol. Spectrosc.* **1988**, *132*, 492–544.